RESEARCH ARTICLE
doi: 10.2306/scienceasia1513-1874.2025.070

ScienceAsia 51 (4): 2025: ID 2025070: **1–10**

Hydroxysafflor yellow A attenuates oxLDL-induced tissue factor in monocytes and reduces thrombosis in dyslipidemic rats

Yangyang Wang[a,*], Xinyao Ren[a], Hui Li[b], Peng Wan[a], Qianchen Wang[a], Jingyan Wang[a,*], Yingjian Hou[c,*]

[a] Affiliated Hospital of Hebei University, Baoding, Hebei 071000 China
[b] Xiong'an Xuanwu Hospital, Baoding, Hebei 071000 China
[c] Hebei University, Baoding, Hebei 071000 China

*Corresponding authors, e-mail: wangyangyang2019@126.com, hdfywjy@sina.com, houyingjian@126.com

Received 10 Jun 2024, Accepted 22 Jul 2025
Available online 30 Aug 2025

ABSTRACT: Safflower, a traditional Chinese herbal medicine, has been approved in China for the treatment of patients with thrombotic cardiovascular events. However, the exact mechanisms by which this herbal medicine protects against these diseases remain elusive. Hydroxysafflor yellow A (HSYA) is a major component of Safflower. Tissue factor (TF) plays a pivotal role in thrombosis formation and propagation. In this study, oxidized low-density lipoprotein (oxLDL)-challenged monocytic THP-1 cells were pretreated with HSYA alone or in combination with 2-chloro-5-nitro-N-phenylbenzamide (GW9662), a peroxisome proliferator-activated receptor-γ (PPARγ) antagonist. Then, TF, PPARγ and phospho-p38 MAPK levels were assessed by real-time PCR and Western blot. In addition, HSYA or HSYA plus GW9662 were administered to rats fed a high-fat diet (HFD) for 4 weeks, and TF, PPARγ and phospho-p38 MAPK levels in peripheral blood mononuclear cells (PBMCs) were evaluated, as well as plasma lipids and thrombus formation were measured. The results showed that HSYA pretreatment reversed oxLDL-induced TF expression and p38 MAPK phosphorylation, and promoted PPARγ expression and activity in THP-1 cells. Plasma lipid and oxLDL amounts were elevated in HFD-fed rats. Although failing to change lipid profile, HSYA reduced TF expression, p38 MAPK phosphorylation, thrombus formation, and promoted PPARγ expression and activity in dyslipidemic rats. GW9662 abolished the effects of HSYA in monocytes. The results indicated that HSYA attenuates oxLDL-induced TF expression in monocytes, and reduces arterial and venous thrombus formation in dyslipidemic rats. These effects of HSYA are likely dependent on PPARγ upregulation and subsequent p38 MAPK inhibition.

KEYWORDS: hydroxysafflor yellow A, tissue factor, thrombosis, peroxisome proliferator-activated receptor γ

INTRODUCTION

Tissue factor (TF), also known as coagulation factor III or thrombokinase, is a key initiator of the extrinsic coagulation cascade. TF binds to coagulation factor VII (FVIIa) with high affinity [1]. The resulting TF-FVIIa complex catalyzes the activation of factor X, which in turn, catalyzes the conversion of prothrombin to thrombin, ultimately leading to blood coagulation and thrombus formation. TF is inducibly or constitutively expressed at high levels in multiple cell types, including endothelial cells, vascular smooth muscle cells, lymphocytes, and monocytes. Under normal conditions, TF is barely present in monocytes. However, monocytic TF expression is dramatically upregulated in several disorders, such as oxidative stress, inflammation, and dyslipidemia [2]. Owens and colleagues demonstrated that monocytic TF is upregulated by increased plasma oxidized low-density lipoprotein (oxLDL), and enhances thrombosis in dyslipidemic humans and animals [3]. Therefore, it could be expected that agents reducing TF or oxLDL would protect against dyslipidemia-induced thrombosis. As a traditional Chinese herbal medicine, safflower (*Carthamus tinctorius* L.) is believed to invigorate the blood, release stagnation, and promote circulation and menstruation. Currently, this herb has been approved in China for the treatment of patients with ischemic cardiovascular diseases. However, the exact mechanisms underlying its protective effects against diseases remain unclear. Several active ingredients have been extracted from *C. tinctorius* L., including yellow and red pigments. Hydroxysafflor yellow A (HSYA), a water-soluble monomeric component, is the main chemical component among the yellow pigments, with multiple biological effects [4, 5]. In addition, Wang and colleagues reported that HSYA effectively inhibits oxidative stress in the liver via upregulation of some antioxidant enzymes [6]. Oxidative stress and inflammation are closely related to dyslipidemia, which is considered a key risk factor for cardiovascular diseases [7–9]. In patients with dyslipidemia and cardiovascular diseases, higher levels of oxidative agents as well as inflammatory mediators are present in the blood [10–12], which induces TF expression and thrombus formation. In the present study, we assessed the effects of HSYA on TF expression, plasma lipid profile, and thrombogenesis.

MATERIALS AND METHODS

Antibodies and reagents

HSYA was obtained commercially from Must Biotechnology Co., Ltd. (Chengdu, China) and human oxLDL from XINYUANJIAHE Biotechnology Co., Ltd. (Beijing, China). Rabbit polyclonal antibodies against TF, β-actin, peroxisome proliferator-activated receptor γ (PPARγ), as well as horseradish peroxidase (HRP)-conjugated anti-rabbit and anti-mouse secondary antibodies were purchased from Santa Cruz Biotechnology (CA, USA). Mouse monoclonal antibodies against p38 MAPK and phospho-p38 MAPK were from Cell Signaling Technology (Beverly, MA, USA). GW9662 was purchased from Sigma-Aldrich (St. Louis, MO, USA).

Cell culture and rat peripheral blood mononuclear cell (PBMC) isolation

The human monocytic leukemia THP-1 cell line was kindly provided by Prof. Yingjian Hou (Hebei University, China). THP-1 cells were cultured in RPMI 1640 (GIBCO, Carlsbad, CA, USA) supplemented with 10% fetal bovine serum (FBS), antibiotic/anti-mycotic, and L-glutamine (GIBCO) at 37 °C in a humidified atmosphere with 5% CO_2. After equilibration in medium containing 2% serum overnight, the cells were used for experiments.

PBMCs were isolated from rat blood samples, as previously reported [13]. Peripheral blood samples were collected with heparin in NaCl (0.9%) as anticoagulant, and diluted with phosphate buffered saline (PBS). The resulting cell suspension was layered over Bandicoot Percoll (Solarbio, Beijing, China). After centrifuged at 1,800×*g* for 30 min, the fraction containing the PBMCs was carefully collected. Subsequently, PBMCs were washed with PBS and resuspended in RPMI 1640 supplemented with 10% FBS. Cell viability was assessed by trypan blue exclusion, and exceeded 95%.

RNA extraction and real-time polymerase chain reaction (PCR)

For assessing mRNA level by real-time PCR, total RNA was extracted from human THP-1 cells and rat PBMCs using TRIzol reagent (Life Technologies, Carlsbad, USA). After quantification, RNA was reverse-transcribed to complementary DNA (cDNA) using a first strand synthesis kit (Thermo Scientific, Rockford, IL, USA). Amplification was performed in a total volume of 25 µl comprising the cDNA template, primers, SYBR Green and EasyTaq PCR Mix (Transgen Biotech, Beijing, China).

Real-time PCR was performed on a MX3000P qPCR detection system (Stratagene, Santa Clara, CA, USA). Relative mRNA amounts were calculated by the comparative threshold cycle method. Gene expression was normalized to β-actin levels.

Western blot analysis

Cells were lysed in lysis buffer (150 mM NaCl, 1% Triton X-100, 100 mM Tris-HCl (pH 7.4), 1 mM EDTA, 1 mM phenylmethylsulfonyl fluoride, 10 µg/ml aprotinin, 10 µg/ml pepstatin A, 20 mM $Na_2P_2O_4$ and 2 mM Na_3VO_4). Total protein was extracted and quantified using a BCA protein assay kit (Pierce Biotechnology Inc., Rockford, USA). Equal amounts of protein were separated by 10% SDS-PAGE, and transferred onto PVDF membranes (Millipore Co., Bedford, MA, USA). The membranes were sequentially incubated with specific primary antibodies and appropriate HRP-conjugated secondary antibodies. Immunoreactive protein bands were visualized by enhanced chemiluminescence (Engreen Biosystem, Beijing, China).

PPARγ transcriptional activity assessment

The transcriptional activity of PPARγ was assessed using a PPARγ transcription factor assay kit (Abcam, Cambridge, USA). Nuclear extracts from THP-1 cells and PBMCs were prepared with the nuclear extraction kit (Abcam), according to the manufacturer's instructions. Then, 100 µg of nuclear extract was added to each well of a 96-well plate pre-coated with a specific double-stranded DNA (dsDNA) sequence containing the peroxisome proliferator response element (PPRE). Specific primary antibodies directed against PPARγ were added, followed by HRP-conjugated secondary antibodies. Absorbance was measured at 450 nm on a microplate reader.

Animal treatment and plasma lipid analysis

Male Sprague-Dawley (SD) rats weighing 180–210 g were purchased from SPF Laboratory Animal Technology Co., Ltd. (Beijing, China), and housed under a natural light/dark cycle (12:12) at 25 °C with food and water ad libitum. Rats were randomly assigned to five groups ($n = 7$ per group): (1) Normal control (NC) group maintained on standard chow; (2) High-fat diet (HFD) model group; (3) HFD + low-dose HSYA (25 mg/kg/day); (4) HFD + medium-dose HSYA (50 mg/kg/day); and (5) HFD + high-dose HSYA (100 mg/kg/day). After a 1-week acclimatization period, groups 2–5 were fed a high-fat diet (D12451, Research Diets, Inc., New Brunswick, USA) for 4 weeks, while the NC group continued receiving standard chow (D12450B, Research Diets). The D12451 HFD was specifically formulated to induce obesity and metabolic dysregulation in rodents, with 45% of total calories derived from fat. Its macronutrient composition consisted of 24% protein (20% kcal), 41% carbohydrate (35% kcal), and 24% fat (45% kcal), yielding an energy density of 4.73 kcal/g. The lipid component comprised primarily lard (88% of total fat content; 177.5 g per 4057 kcal) supplemented with soybean oil (12% of total fat; 25 g per 4057 kcal). The diet contained 196.5 mg cholesterol per kg, predominantly derived from lard (0.95 mg/g).During the last two weeks, HFD fed rats were injected intraperitoneally with vehicle or HSYA (25, 50, and 100 mg/kg/day, respectively). After 2 weeks of treatment, the rats were anesthetized, and body weights measured; blood was collected for biochemical analysis. All experimental procedures were conducted in accordance with the Guide for the Care and Use of Laboratory Animals by the US National Institutes of Health (NIH Publication No. 85-23, revised 1996); the animal experimental protocol was approved by the Institutional Animal Care and Use Committee of Hebei University.

Plasma triglyceride and cholesterol levels were determined with an automated clinical chemistry analyzer kit (Biosino Biotech, Beijing, China). The plasma levels of high-density lipoprotein (HDL), low-density lipoprotein (LDL), apolipoprotein A1 (APOA1), and apolipoprotein B (APOB) were measured using an automated clinical chemistry analyzer with matched reagent kits (Dirui Medical Technology Co., Ltd., Changchun, China). An ELISA kit (RD System, Minneapolis, MN, USA) was used to measure plasma oxLDL levels, according to the manufacturer's instructions.

Establishment of a carotid artery thrombosis model

The rats were randomly assigned to four experimental groups ($n = 7$ per group): (1) Normal control group fed standard chow diet (D12450B, Research Diets, Inc.); (2) HFD model group receiving D12451 diet (Research Diets, Inc.; 45% kcal from fat) and vehicle injections; (3) HFD + HSYA treatment group (50 mg/kg/day, i.p.); (4) HFD + HSYA (50 mg/kg/day) + GW9662 (1 mg/kg/day, i.p.) combination treatment group. Following a 1-week acclimation period, dyslipidemia was induced by 4 weeks of HFD feeding in groups 2–4. Pharmacological interventions were administered during the final 2 weeks of dietary induction, with all injections performed at consistent times daily. The normal control group received standard diet throughout the study period without any pharmacological treatment. Four hours after the last treatment, the animals were anesthetized with pentobarbital sodium (100 mg/kg, DINGGUO, Beijing, China). Then, the left common carotid artery was dissected and a stack of filter paper was saturated with ferric chloride (10% w/v) and placed on the adventitia's surface. After 3 min, blood flow of the carotid artery was monitored on a flowmeter (Transonic Systems, Ithaca, NY, USA), and time to occlusion was measured.

Venous thrombosis model establishment

Ligation of inferior vena cava (IVC) was performed to induce venous thrombosis as described previously [14]. Before IVC ligation, rats were fed HFD for 4 weeks. During the last two weeks, dyslipidemic rats were injected daily with vehicle, HSYA (50 mg/kg/day) or HSYA (50 mg/kg/day) plus GW9662 (1 mg/kg/day). After 2 weeks of treatment, rats were anesthetized with pentobarbital sodium (50 mg/kg, DINGGUO). A midline laparotomy was performed, with the IVC ligated immediately below the renal veins. The abdomen was closed and the animal was allowed to recover. After 7 days, the IVC was harvested and weighed; the resulting weights were normalized to body weight (mg/kg) to derive the mass of thrombus formed during the period of venous stasis.

Statistical analysis

Statistical analysis was conducted using GraphPad Prism version 10.1. Data are presented as mean ± standard deviation (SD) and represent results from at least three independent experiments. The normality of the data was assessed using the Shapiro-Wilk test. For normally distributed data, one-way analysis of variance (ANOVA) was employed to compare differences among groups. When ANOVA indicated significant differences, post hoc multiple comparisons were conducted using Tukey's test. $p < 0.05$ was considered statistically significant. Significant differences between groups are indicated in the figure legends.

RESULTS

HSYA inhibits oxLDL-induced TF expression in human monocytic THP-1 cells

To investigate whether HSYA modulates TF expression in monocytes, THP-1 cells were pretreated with HSYA at various concentrations for 4 h, and challenged with oxLDL (50 µg/ml). Real-time PCR was then used to determine TF mRNA levels. The results showed that OxLDL stimulation markedly increased TF mRNA expression in THP-1 cells. Compared with cells treated with oxLDL alone, pretreatment with HSYA at 0.2 µM and 1 µM reduced TF mRNA levels by approximately 49% and 64%, respectively (Fig. 1A). However, 0.04 µM of HSYA only displayed a modest inhibitory effect on TF expression. Subsequently, TF protein levels were measured by Western blot. As shown in Fig. 1B and C, oxLDL-induced TF protein expression was also effectively attenuated by HSYA at 0.2 µM and 1 µM but not 0.04 µM. These findings indicated that HSYA suppresses monocytic TF expression.

HSYA inhibits TF induction by oxLDL in THP-1 cells by enhancing PPARγ activity and reducing p38 MAPK phosphorylation

As a nuclear receptor, PPARγ is activated by binding to its ligands, and promotes its own transcription as well as that of target genes. It was reported previously that HSYA suppresses liver fibrosis via PPARγ upregulation [15]. Similar to the previous report, our data showed that PPARγ transcriptional activity was also enhanced by HSYA at 0.2 µM and 1 µM (Fig. 2A). Cells were pretreated with HSYA or HSYA plus GW9662, a PPARγ-specific inhibitor, for 4 h. Subsequently, THP-1 cells were challenged with oxLDL. HSYA-enhanced PPARγ activity was suppressed partially by GW9662 pretreatment (Fig. 2B). Using real-time PCR, the mRNA level of TF was measured in THP-1 cells. As shown in Fig. 2C, oxLDL-induced

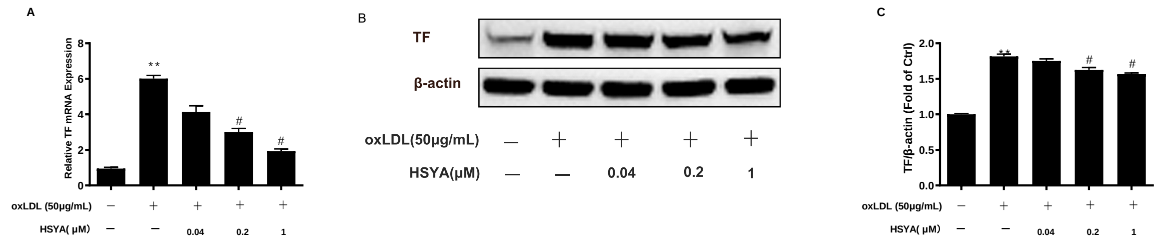

Fig. 1 HSYA suppresses oxLDL-induced TF expression in monocytic THP-1 cells. Followed by oxLDL challenge (50 µg/ml), THP-1 cells were pretreated with HSYA at the indicated doses for 4 h. Then, mRNA (A) and protein (B) levels of TF were determined by real-time PCR and Western blot, respectively. Densitometric analysis of Western blot bands was performed using ImageJ software (C). All experiments were performed in triplicate. $^{**}p < 0.01$ vs. untreated cells; $^{\#}p < 0.05$ vs. cells treated with oxLDL alone.

TF mRNA expression was inhibited by HSYA pre-incubation, which was at least partially reversed by GW9662. Similar patterns of TF protein expression were observed in Western blot analyses (Fig. 2D, E). These results indicated that PPARγ activation may be responsible for the inhibitory effects of HSYA on TF expression.

The MAPK pathway mediates NF-κB-dependent TF expression, and PPARγ activation can inhibit MAPK phosphorylation and activity [16, 17]. To assess the regulation of MAPK activity by HSYA and PPARγ, we examined p38 MAPK phosphorylation in THP-1 cells. As shown in Fig. 2F and G, oxLDL challenge resulted in elevated ratio of phospho/total-p38 MAPK, an effect that was at least partially abolished by HSYA treatment. However, HSYA-suppressed MAPK phosphorylation was blocked by GW9662. The PPARγ specific inhibitor also decreased HSYA-suppressed TF expression. These results suggested that p38 MAPK may be downstream of PPARγ which mediates the inhibitory effects of HSYA on TF expression.

HSYA fails to improve the plasma lipid profile in rats fed high-fat diet

To extend our *in vitro* observations to an *in vivo* context, a dyslipidemic animal model was established with rats fed HFD for 4 weeks. From weeks 3 to 4, the animals were injected intraperitoneally with vehicle or HSYA (25, 50 and 100 mg/kg/day). Compared to rats fed a normal chow diet, the plasma levels of LDL, APOB, oxLDL, total cholesterol, and triglycerides were significantly higher in HFD-fed rats, while HDL and APOA1 levels were lower (Fig. 3). In addition, the HFD greatly accelerated weight gain in rats. However, no significant differences in body weight and blood lipids levels were detected between untreated dyslipidemic rats and those treated with various doses of HSYA.

HSYA suppresses TF expression in dyslipidemic rats by upregulating PPARγ and suppressing p38 MAPK phosphorylation

The aforementioned animal models were used to confirm our *in vitro* findings that HSYA inhibits TF expression by enhancing PPARγ activity and suppressing MAPK phosphorylation. Compared with PBMCs isolated from normal control rats, higher levels of p38 MAPK phosphorylation and TF expression were observed in cells from dyslipidemic rats (Fig. 4B–F). As shown in Fig. 4, HSYA administration attenuated dyslipidemia-induced p38 MAPK phosphorylation and TF expression, and enhanced PPARγ transcriptional activity. All these responses of PBMCs to HSYA were blocked by GW9662 treatment (1 mg/kg/day, intraperitoneally). Therefore, these *in vivo* data further confirmed the inhibitory effects of HSYA on TF expression via activation of PPARγ and suppression of p38 MAPK phosphorylation.

HSYA attenuates thrombus formation accelerated by dyslipidemia in rats

TF is a predominant activator of blood coagulation and thrombus formation. To assess the functional consequence of HSYA regulation of TF, venous and arterial thrombus formation was assessed. The common carotid artery was damaged with 10% $FeCl_3$, inducing thrombosis that led to vessel occlusion. Compared with HFD-fed rats injected with vehicle, time to occlusion of the damaged artery was prolonged in HSYA-treated HFD rats (Fig. 5A). This indicated that HSYA was capable of delaying arterial thrombus formation. Meanwhile, the effect of HSYA on arterial thrombus formation was abolished, at least in part, by GW9662 treatment (1 mg/kg/day). IVC ligation was employed to induce deep vein thrombosis. Similarly, HSYA exhibited an inhibitory effect on the venous thrombus mass, an effect blocked by GW9662 (Fig. 5B).

DISCUSSION

Thrombus, a blood clot that develops in blood vessels, can obstruct the blood flow to major organs and induce cardiovascular diseases [18]. As noted by Chananikan et al [19], acute coronary syndrome (ACS) is a group of symptoms with high morbidity and mortality, often caused by the erosion or rupture of atherosclerotic plaques. The pathology begins with plaque formation in the coronary arteries, and elevated

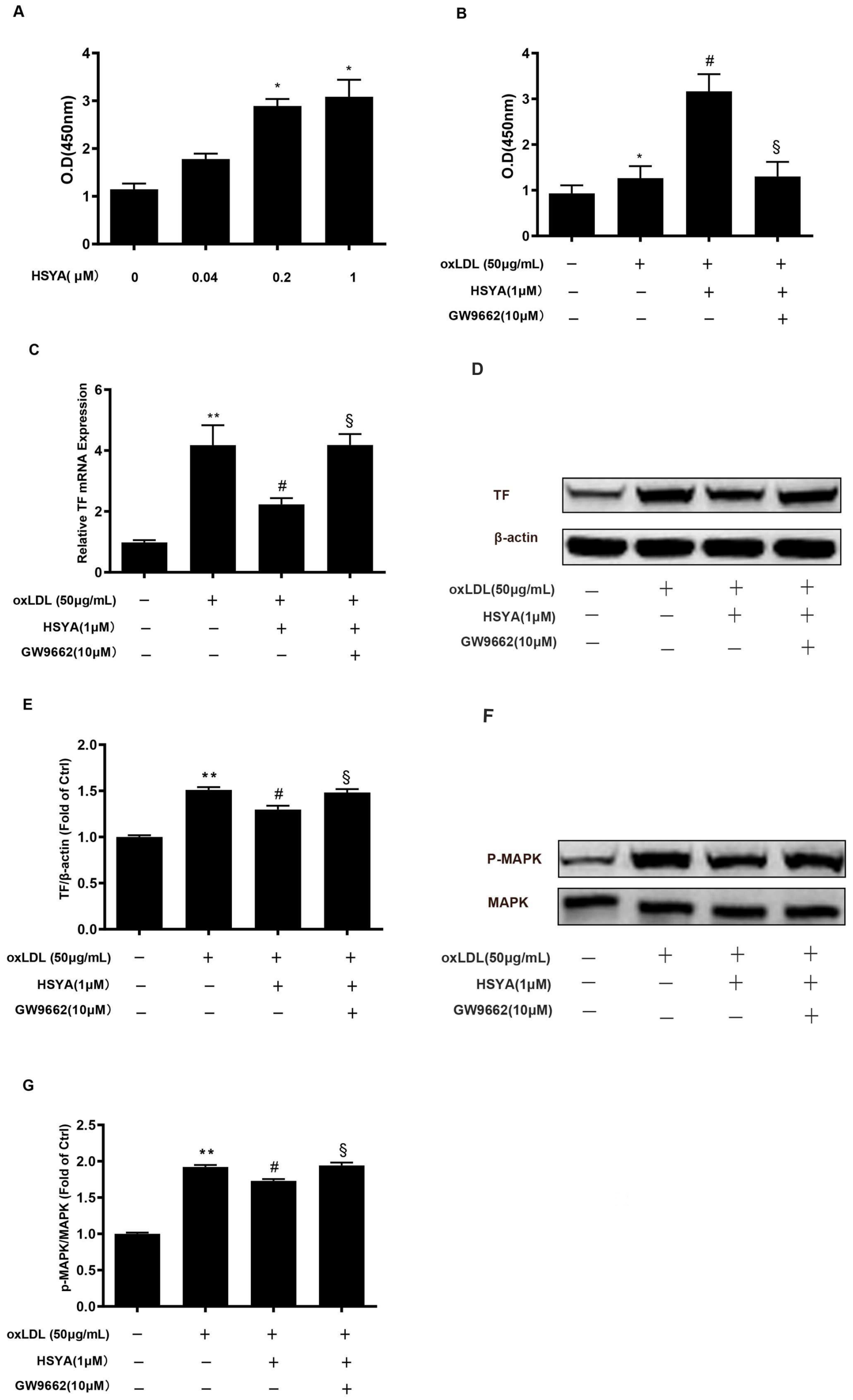

Fig. 2 HSYA suppresses TF expression through the PPARγ/MAPK pathway. THP-1 cells were incubated with HSYA at the indicated doses for 4 h. PPARγ transcriptional activity was determined with a transcription factor assay kit (A). Followed by oxLDL challenge (50 µg/ml), THP-1 cells were pretreated with HSYA (1 µM) alone or in combination with GW9662 (10 µM) for 4 h. PPARγ activity (B), TF at the levels of mRNA (C) and protein (D, E), and MAPK phosphorylation (F, G) were detected. Densitometric analysis of Western blot bands was performed using ImageJ software (E, G). All experiments were performed in triplicate. $^{**}p < 0.01$ vs. untreated cells; $^{\#}p < 0.05$ vs. cells treated with oxLDL alone; $^{\S}p < 0.05$ vs. cells treated with oxLDL plus HSYA.

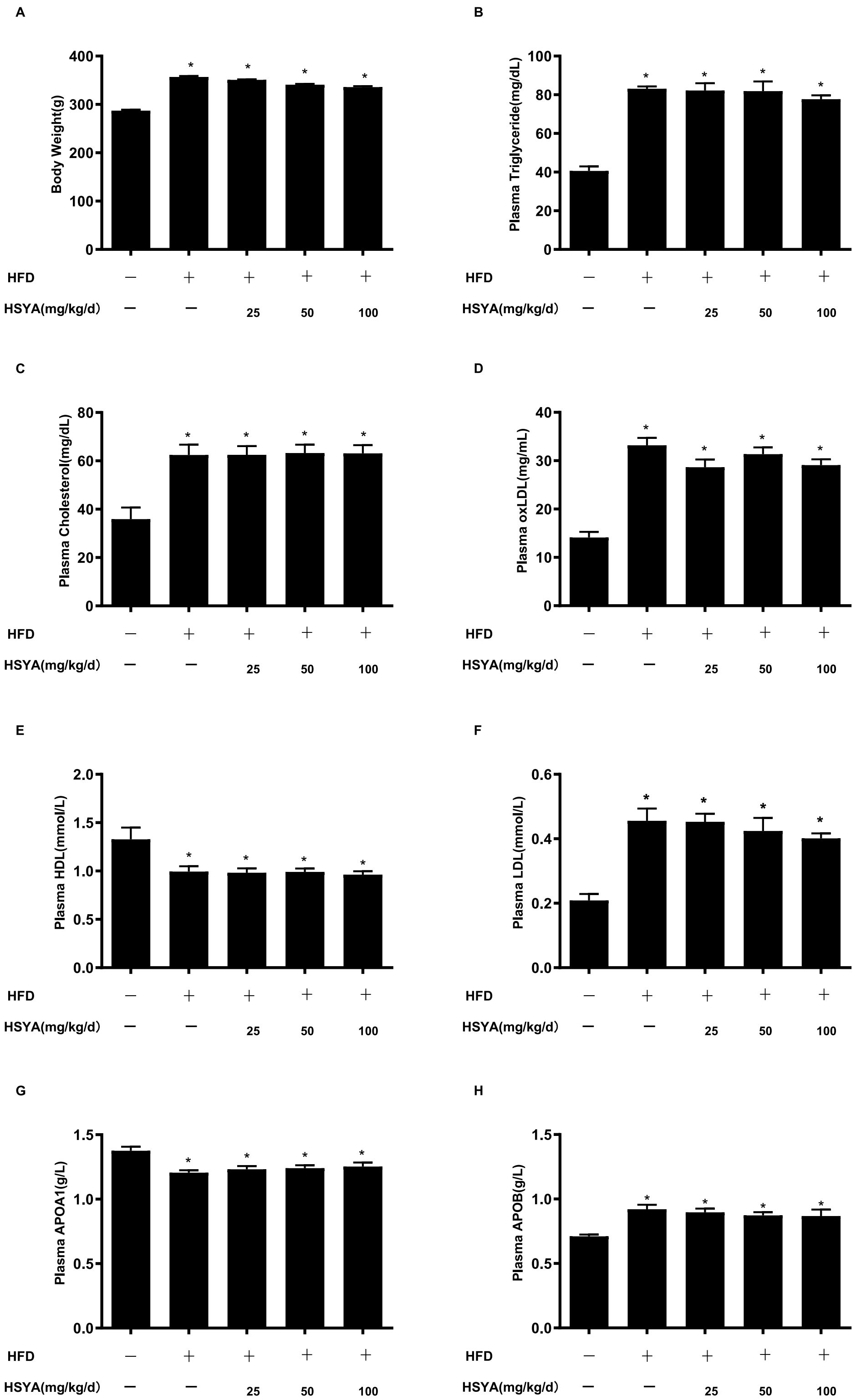

Fig. 3 HSYA does not improve the plasma lipid profile in rats fed a high-fat diet (HFD). Rats were fed a rodent chow diet or HFD for 4 weeks. During the last two weeks, HFD-fed rats were injected intraperitoneally with vehicle or HSYA (25, 50, 100 mg/kg/day). After 2 weeks of administration, rat body weights were measured, and blood was drawn to determine total triglyceride (TG), total cholesterol (TC), oxLDL, LDL, HDL, APOA1 and APOB levels in the plasma. Histobars represent mean ± SD ($n = 7$). $^*p < 0.05$ vs. chow diet group.

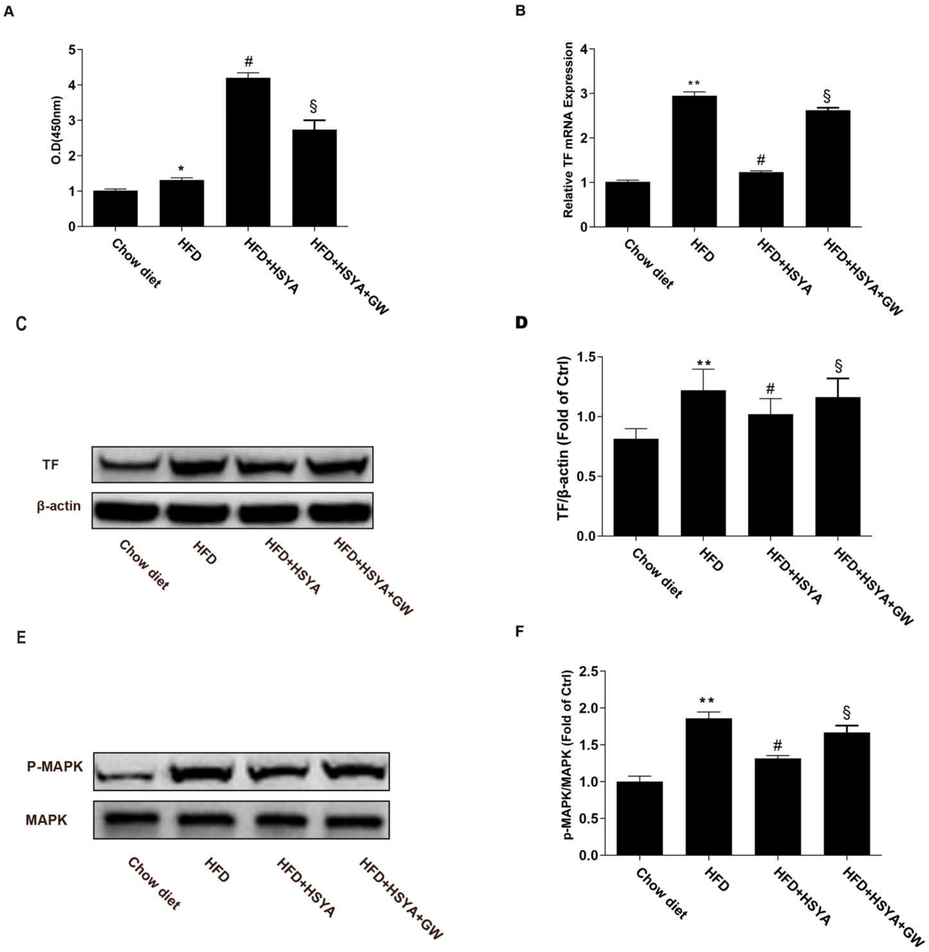

Fig. 4 HSYA attenuates TF induction in dyslipidemic rats via the PPARγ/MAPK pathway. Rats were fed a chow diet or HFD for 4 weeks. During the last two weeks, dyslipidemic rats were injected intraperitoneally with vehicle, HSYA (50 mg/kg/day) or HSYA (50 mg/kg/day) plus GW9662 (1 mg/kg/day). Six hours after the last treatment, PPARγ transcriptional activity was determined with a transcription factor assay kit (A). TF mRNA level were assessed by real-time PCR (B). TF protein (C, D) and MAPK phosphorylation levels (E, F) were detected by Western blot. Densitometric analysis of Western blot bands was performed using ImageJ software (D, F). PPARγ transcriptional activity was determined with a transcription factor assay kit. Histobars represent mean ± SD ($n = 7$). $^{*} p < 0.05$, $^{**} p < 0.01$ vs. chow diet group. $^{\#} p < 0.05$ vs. HFD group; $^{\S} p < 0.05$ vs. HFD+HSYA.

inflammatory biomarkers, such as fibrinogen and hs-CRP, are linked to plaque progression and rupture, ultimately leading to thrombus formation and cardiovascular events. TF plays a pivotal role in the formation and propagation of thrombosis. With a cell type-specific deletion approach, Pawlinski and Mackman analyzed the cellular sources of TF that contribute to coagulation activation. They found that TF expression by both bone marrow and non-bone marrow cells promotes coagulation. Myeloid cells (most likely monocytes) are the major source of TF amongst bone marrow cells [20]. HSYA is a major active chemical component of safflower, which is used for the treatment of cardiovascular diseases in China. However, the mechanisms underlying the effects of safflower on cardiovascular diseases remain unclear. In the present study, HSYA attenuated the induction of monocytic TF by oxLDL and reduced thrombosis in dyslipidemic rats.

PPARγ has been shown to be implicated in HSYA's effects. Similar to the way re-searchers study the physicochemical properties and engine performance of biodiesel from egusi seeds [21], we utilized biochemical and molecular biology techniques to explore the mechanisms underlying HSYA's effects on cardiovascular diseases. Liu et al demonstrated that HSYA reduces CCl_4- and HFD-mediated liver fibrosis via PPARγ upregulation [22, 23]. PPARs belong to the nuclear receptor superfamily that functions as transcription factors regulating the expression of their target genes [24]. Activated by their respective ligands, PPARs heterodimerize with the retinoid X receptor (RXR) and bind to specific regions on target

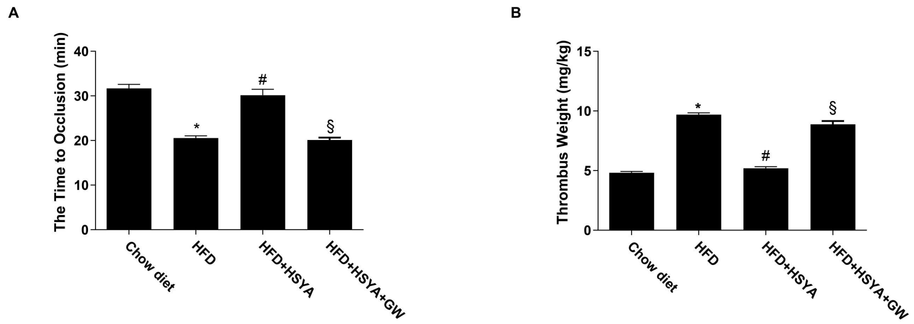

Fig. 5 Effects of HSYA administration on thrombogenesis. Rats were fed a chow diet or HFD for 4 weeks. During the last two weeks, dyslipidemic rats were injected intraperitoneally with vehicle, HSYA (50 mg/kg/day) or HSYA (50 mg/kg/day) plus GW9662 (1 mg/kg/day). Six hours after the last treatment, the left common carotid artery was stimulated with ferric chloride (10% w/v), and time to artery occlusion was measured (A). Ligation of the inferior vena cava (IVC) was performed to induce venous thrombosis. After 7 days, the IVC was extracted and weighed; the weights were normalized to body weights (mg/kg) to calculate the mass of thrombus formed during the period of venous stasis (B). Histobars represent mean ± SD ($n = 7$). $^{*}p < 0.05$ vs. chow diet group, $^{\#}p < 0.05$ vs. HFD rats treated with vehicle.

gene DNAs. There are 3 known PPAR isoforms in mammals, namely α, β/δ, and γ. PPARγ plays an essential role in various physiological and pathological processes such as adipogenesis, insulin resistance, and inflammation [24]. In addition, PPARγ exhibits a close association with thrombus formation and TF expression. Although Neri et al proposed that PPARγ agonists could promote thrombogenesis by increasing TF-bearing microparticles [25, 26], further studies demonstrated the inhibitory effects of PPARγ on TF and thrombosis. In human vascular endothelial cells and monocytes, TF induction in response to TNF-α is inhibited by rosiglitazone, a synthetic PPARγ agonist [27, 28]. As shown above, HSYA enhanced the expression and transcriptional activity of PPARγ in human THP-1 cells and rat PBMCs. In addition, a PPARγ antagonist abolished HSYA induced inhibition of both monocytic TF expression and thrombus formation. These results suggest that PPARγ upregulation could be a prerequisite for the inhibitory effects of HSYA on TF and thrombosis.

In addition to PPARγ, p38 MAPK is involved in HSYA's effect on TF expression. As shown in the study of geniposidic acid [29], which exhibits anti-inflammatory properties and can suppress inflammation by regulating various proteins, our research also suggests that HSYA's inhibitory effects on TF and thrombosis may involve multiple signaling pathways. Of note, p38 MAPK is phosphorylated and activated by a diverse array of stimuli such as mitogens and inflammatory cytokines. Hu et al demonstrated that oxLDL induces p38 MAPK phosphorylation and activation [30, 31], in agreement with our results. Meanwhile, p38 MAPK activation plays an essential role in TF expression induced by platelet-derived growth factor (PDGF), endotoxin and phosphatidylserine-dependent anti-prothrombin anti-body [32]. PPARγ is upstream to MAPK. Liu et al reported that HSYA upregulates PPARγ expression and reduces p38 MAPK phosphorylation, effects abolished by the PPARγ antago-nist GW9662. Concurrent to reduced TF expression, we found that HSYA suppressed p38 MAPK phosphorylation in oxLDL-challenged THP-1 cells and dyslipidemic rats, and these effects were blocked by GW9662. These results suggest that PPARγ upregulation suppresses TF expression by blocking p38 MAPK activation in HSYA-treated monocytes.

Dyslipidemia affects millions of patients worldwide, who have elevated levels of plas-ma lipids consisting largely of triglycerides and cholesterol (and derived esters). It is well established that elevated triglyceride and cholesterol amounts in plasma contribute greatly to a higher prevalence of arterial thrombosis [33, 34]. In this study, accelerated arterial and venous thrombosis was found to parallel elevated levels of plasma triglycerides, cholesterol, and oxLDL in HFD-fed rats. Compared with untreated dyslipidemic rats, HSYA at 50 mg/kg/day barely improved the lipid profile. In the above *in vivo* experiments, the HSYA dosage used was similar to or even higher than those previously reported. It was suggested that 50 mg/kg/-day of HSYA is sufficient to improve pulmonary fibrosis, and lipopolysaccharide-induced inflammation was effectively inhibited by HSYA at 40 mg/kg/day [35, 36]. Although regular HSYA doses have no effects on plasma lipids, HSYA at 50 mg/kg/day significantly suppressed monocytic TF expression as well as arterial and venous thrombus formation in dyslipidemic rats. These results suggest that HSYA suppression of thrombosis could be independent of its hypolipidemic effects. We propose that the inhibitory effects of HSYA on dyslipidemic-enhanced thrombosis may be attributed to oxLDL downregulation-induced TF. Several studies demonstrated that oxLDL, in dyslipidemia setting, induces TF expression and thrombosis in human monocytes, which is consistent with the present data [37, 38]. The TF-FVIIa complex catalyzes factor X activation, leading to thrombin generation, and finally a fibrin clot. Reduced TF activity with neutralizing antibodies greatly im-proves the coagulation status in dyslipidemic mice, and TF deficiency in myeloid cells limits thrombogenesis [39]. Therefore, dyslipidemia-related thrombosis can be improved by HSYA, which was shown to suppress hematopoietic cell-derived TF in the present study. Certainly, other mechanisms involved in HSYA inhibition of thrombosis cannot be ruled out.

The clinical significance of this study extends beyond providing new strategies for the treatment of thrombotic diseases. It also offers new insights for the development of HSYA-based pharmaceutical therapies. Given that hyperlipidemia exacerbates thrombosis, targeting TF expression with HSYA could offer an effective treatment option for arterial and venous thromboembolic events. Furthermore, HSYA's ability to regulate key signaling pathways such as PPARγ and p38 MAPK provides a foundation for the development of novel multi-targeted therapeutic strategies for thrombotic diseases.

Although the results of our study are promising, several limitations need to be addressed in future research. First, while we have demonstrated the inhibitory effects of HSYA on TF expression and thrombosis in animal models, these findings need to be confirmed in human clinical trials to assess their translational relevance. The dose of HSYA used in our study was relatively high, and future research should explore optimal dosing strategies and evaluate the long-term safety of HSYA in humans. Furthermore, although our research focused on the impact of HSYA on TF expression in a hyperlipidemic rat model, the broader effects of HSYA on platelet function, coagulation pathways, and endothelial cell behavior have not been fully explored. Future studies should investigate these aspects to provide a more comprehensive understanding of HSYA's role in thrombosis. Further exploration of how HSYA interacts with other thrombotic mediators, such as fibrinogen or prothrombin, may also reveal its therapeutic potential. Finally, while our study suggests that HSYA reduces thrombotic events independently of its lipid-lowering effects, investigating the interactions between HSYA and other anti-thrombotic drugs (such as anticoagulants or antiplatelet drugs) is essential. Research on potential drug interactions will help determine the safety and efficacy of HSYA as part of a comprehensive treatment strategy for thrombotic diseases.

CONCLUSION

We demonstrated that HSYA attenuates oxLDL-induced TF expression in monocytes, and reduces arterial and venous thrombus formation in dyslipidemic rats. These protective effects of HSYA are possibly dependent on PPARγ activation and subsequent p38 MAPK inhibition. These findings suggest that HSYA could be developed as a novel therapeutic approach for the treatment of thrombotic diseases.

Acknowledgements: We would like to express our gratitude to all those who helped us during the writing of this manuscript. Thanks to all the peer reviewers for their opinions and suggestions. Funding: (1) The Natural Science Foundation of Hebei Province of China (H2023201022). (2) Government Foundation of Clinical Medicine Talents Training Program of Hebei Province (361007).

REFERENCES

1. Grover SP, Mackman N (2018) Tissue factor: An essential mediator of hemostasis and trigger of thrombosis. *Arterioscler Thromb Vasc Biol* **38**, 709–725.
2. Owens AP 3rd, Byrnes JR, Mackman N (2014) Hyperlipidemia, tissue factor, coagulation, and simvastatin. *Trends Cardiovasc Med* **24**, 95–98.
3. Otomo K, Amengual O, Fujieda Y, Nakagawa H, Kato M, Oku K, Horita T, Yasuda S, et al (2016) Role of apolipoprotein B100 and oxidized low-density lipoprotein in the monocyte tissue factor induction mediated by anti-β2 glycoprotein I antibodies. *Lupus* **25**, 1288–1298.
4. Ao H, Feng W, Peng C (2018) Hydroxysafflor yellow A: A promising therapeutic agent for a broad spectrum of diseases. *Evid Based Complement Alternat Med* **2018**, 8259280.
5. Bai X, Wang WX, Fu RJ, Yue SJ, Gao H, Chen YY, Tang YP (2020) Therapeutic potential of hydroxysafflor yellow A on cardio-cerebrovascular diseases. *Front Pharmacol* **11**, 01265.
6. Yan K, Wang X, Pan H, Wang L, Yang H, Liu M, Zhu H, Gong F (2020) Safflower yellow and its main component HSYA alleviate diet-induced obesity in mice: Possible involvement of the increased antioxidant enzymes in liver and adipose tissue. *Front Pharmacol* **11**, 482.
7. Feillet-Coudray C, Fouret G, Vigor C, Bonafos B, Jover B, Blachnio-Zabielska A, Rieusset J, Casas F, et al (2019) Long-term measures of dyslipidemia, inflammation, and oxidative stress in rats fed a high-fat/high-fructose diet. *Lipids* **54**, 81–97.
8. Kalita S, Khandelwal S, Madan J, Pandya H, Sesikeran B, Krishnaswamy K (2018) Almonds and cardiovascular health: A review. *Nutrients* **10**, 468.
9. Farzanegi P, Dana A, Ebrahimpoor Z, Asadi M, Azarbayjani MA (2019) Mechanisms of beneficial effects of exercise training on non-alcoholic fatty liver disease (NAFLD): Roles of oxidative stress and inflammation. *Eur J Sport Sci* **19**, 994–1003.
10. Padró T, Vilahur G, Badimon L (2018) Dyslipidemias and microcirculation. *Curr Pharm Des* **24**, 2921–2926.
11. Ganjali S, Gotto AM Jr, Ruscica M, Atkin SL, Butler AE, Banach M, Sahebkar A (2018) Monocyte-to-HDL-cholesterol ratio as a prognostic marker in cardiovascular diseases. *J Cell Physiol* **233**, 9237–9246.
12. Libby P, Mallat Z, Weyand C (2021) Immune and inflammatory mechanisms mediate cardiovascular diseases from head to toe. *Cardiovasc Res* **117**, 2503–2505.

13. Fu Y, Hou Y, Fu C, Gu M, Li C, Kong W, Wang X, Shyy JY, et al (2011) A novel mechanism of gamma/delta T-lymphocyte and endothelial activation by shear stress: the role of ecto-ATP synthase beta chain. *Circ Res* **108**, 410–417.
14. Day SM, Reeve JL, Pedersen B, Farris DM, Myers DD, Im M, Wakefield TW, Mackman N, et al (2005) Macrovascular thrombosis is driven by tissue factor derived primarily from the blood vessel wall. *Blood* **105**, 192–198.
15. Liu Q, Wang CY, Liu Z, Ma XS, He YH, Chen SS, Bai XY (2014) Hydroxysafflor yellow A suppresses liver fibrosis induced by carbon tetrachloride with high-fat diet by regulating PPAR-gamma/p38 MAPK signaling. *Pharm Biol* **52**, 1085–1093.
16. He M, He X, Xie Q, Chen F, He S (2006) Angiotensin II induces the expression of tissue factor and its mechanism in human monocytes. *Thromb Res* **117**, 579–590.
17. Li T, Wang W, Zhao JH, Zhou X, Li YM, Chen H (2015) Pseudolaric acid B inhibits T-cell mediated immune response *in vivo* via p38MAPK signal cascades and PPAR-gamma activation. *Life Sci* **121**, 88–96.
18. Alkarithi G, Duval C, Shi Y, Macrae FL, Ariëns RAS (2021) Thrombus structural composition in cardiovascular disease. *Arterioscler Thromb Vasc Biol* **41**, 2370–2383.
19. Makmool C, Pussadhamma B, Leuangwatthananon W, Howhan S, Komanasin N (2022) Fibrinogen with high-sensitivity C-reactive protein: A combined prediction biomarker for acute coronary syndrome risk assessment. *ScienceAsia* **48**, 8–14.
20. Grover SP, Mackman N (2018) Tissue factor: An essential mediator of hemostasis and trigger of thrombosis. *Arterioscler Thromb Vasc Biol* **38**, 709–725.
21. Bande YM, Adam NM, Jamarei BO, Azmi Y, Razali SZ (2013) Examining the physicochemical properties and engine performance of biodiesel from whole seed and extracted kernels of egusi (*Citrullus lanatus*). *ScienceAsia* **39**, 492–499.
22. Liu Q, Wang CY, Liu Z, Ma XS, He YH, Chen SS, Bai XY (2014) Hydroxysafflor yellow A suppresses liver fibrosis induced by carbon tetrachloride with high-fat diet by regulating PPAR-γ/p38 MAPK signaling. *Pharm Biol* **52**, 1085–1093.
23. Wang CY, Liu Q, Huang QX, Liu JT, He YH, Lu JJ, Bai XY (2013) Activation of PPARγ is required for hydroxysafflor yellow A of *Carthamus tinctorius* to attenuate hepatic fibrosis induced by oxidative stress. *Phytomedicine* **20**, 592–599.
24. Wagner N, Wagner KD (2020) The role of PPARs in disease. *Cells* **9**, 2367.
25. Neri T, Cordazzo C, Carmazzi Y, Petrini S, Balìa C, Stefanelli F, Amoruso A, Brunelleschi S, et al (2012) Effects of peroxisome proliferator-activated receptor-γ agonists on the generation of microparticles by monocytes/macrophages. *Cardiovasc Res* **94**, 537–544.
26. Montaigne D, Butruille L, Staels B (2021) PPAR control of metabolism and cardiovascular functions. *Nat Rev Cardiol* **18**, 809–823.
27. Li J, Shen X (2019) Effect of rosiglitazone on inflammatory cytokines and oxidative stress after intensive insulin therapy in patients with newly diagnosed type 2 diabetes. *Diabetol Metab Syndr* **11**, 35.
28. Hollerbach A, Müller-Calleja N, Canisius A, Orning C, Lackner KJ (2020) Induction of tissue factor expression by anti-β2-glycoprotein I is mediated by tumor necrosis factor α. *J Thromb Thrombolysis* **49**, 228–234.
29. Wang G, Qing Y, Zhang Q, Han Z (2023) The proteomic analysis of anti-inflammatory effects of geniposidic acid in LPS induced THP1 monocytic cells. *ScienceAsia* **49**, 411–420.
30. Lu L, Huang J, Xue X, Wang T, Huang Z, Li J (2021) Berberine regulated miR150-5p to inhibit P2X7 receptor, EMMPRIN and MMP-9 expression in oxLDL induced macrophages. *Front Pharmacol* **12**, 639558.
31. Gong L, Lei Y, Liu Y, Tan F, Li S, Wang X, Xu M, Cai W, et al (2019) Vaccarin prevents ox-LDL-induced HUVEC EndMT, inflammation and apoptosis by suppressing ROS/p38 MAPK signaling. *Am J Transl Res* **11**, 2140–2154.
32. Cimmino G, Cirillo P (2018) Tissue factor: newer concepts in thrombosis and its role beyond thrombosis and hemostasis. *Cardiovasc Diagn Ther* **8**, 581–593.
33. Welty FK (2020) Dietary treatment to lower cholesterol and triglyceride and reduce cardiovascular risk. *Curr Opin Lipidol* **31**, 206–231.
34. Miao J, Zang X, Cui X, Zhang J (2020) Autophagy, hyperlipidemia, and atherosclerosis. *Adv Exp Med Biol* **1207**, 237–264.
35. Jin M, Sun CY, Pei CQ, Wang L, Zhang PC (2013) Effect of safflor yellow injection on inhibiting lipopolysaccharide-induced pulmonary inflammatory injury in mice. *Chin J Integr Med* **19**, 836–843.
36. Wang L, Jin M, Zang BX, Wu Y (2011) Inhibitory effect of safflor yellow on pulmonary fibrosis. *Biol Pharm Bull* **34**, 511–516.
37. Cimmino G, Cirillo P, Conte S, Pellegrino G, Barra G, Maresca L, Morello A, Calì G, et al (2020) Oxidized low-density lipoproteins induce tissue factor expression in T-lymphocytes via activation of lectin-like oxidized low-density lipoprotein receptor-1. *Cardiovasc Res* **116**, 1125–1135.
38. Obermayer G, Afonyushkin T, Binder CJ (2018) Oxidized low-density lipoprotein in inflammation-driven thrombosis. *J Thromb Haemost* **16**, 418–428.
39. Owens AP 3rd, Byrnes JR, Mackman N (2014) Hyperlipidemia, tissue factor, coagulation, and simvastatin. *Trends Cardiovasc Med* **24**, 95–98.